JOURNAL OF VIROLOGY, Apr. 2006, p. 3249–3258 Vol. 80, No. 7
0022-538X/06/$08.00+0 doi:10.1128/JVI.80.7.3249–3258.2006

Membrane-Anchored Inhibitory Peptides Capture Human Immunodeficiency Virus Type 1 gp41 Conformations That Engage the Target Membrane prior to Fusion

Gregory B. Melikyan,[1]* Marc Egelhofer,[2] and Dorothee von Laer[2]

Department of Molecular Biophysics and Physiology, Rush University Medical Center, 1653 W. Congress Pkwy., Chicago, Illinois 60612,[1] and Institute for Biomedical Research Georg-Speyer-Haus, Frankfurt, Germany[2]

Received 5 December 2005/Accepted 10 January 2006

Soluble peptides derived from the C-terminal heptad repeat domain of human immunodeficiency virus type 1 (HIV-1) gp41 are potent inhibitors of HIV-1 entry and gp41-induced fusion. Target membrane-anchored variants of these peptides have been shown to retain inhibitory activity. Both soluble and membrane-anchored C peptides (MACs) are thought to block fusion by binding to the N-terminal coiled coil domain of gp41 and preventing formation of the final six-helix bundle structure. However, interactions of target MACs with gp41 must be restricted to a subset of trimers that have their hydrophobic fusion peptides inserted into the target membrane. This unique feature of MACs was used to identify the intermediate step of fusion at which gp41 engaged the target membrane. Fusion between HIV envelope-expressing effector cells and target cells was measured by fluorescence microscopy. Expression of MACs in target cells led to less than twofold reduction in the extent of fusion. However, when reaction was first arrested by adding lysolipids that disfavored membrane merger, and the lipids were subsequently removed by washing, control cells supported fusion, whereas those that expressed MACs did not. The drastically improved potency of MACs implies that, at lipid-arrested stage, gp41 bridges the viral and target cell membranes and therefore more optimally binds the membrane-anchored peptides. Experimental demonstration of this intermediate shows that, similar to fusion induced by many other viral glycoproteins, engaging the target membrane by HIV-1 gp41 permits coupling between six-helix bundle formation and membrane merger.

Human immunodeficiency virus type 1 (HIV-1) envelope (Env) induces fusion between the viral and cell membranes through a multitude of steps. Binding of the surface subunit, gp120, to CD4 permits interaction of gp120 with chemokine receptors (usually CCR5 or CXCR4). Formation of ternary gp120/CD4/coreceptor complexes is thought to trigger conformational changes in the transmembrane gp41 subunit, culminating in formation of a thermodynamically stable six-helix bundle (6HB) structure (Fig. 1). All known structures of the ectodomains of class I viral fusion proteins share a common 6HB motif (15, 38). HIV gp41 6HBs are comprised of the central triple-stranded coiled coil contributed by the three N-terminal heptad repeat domains. Three C-terminal helical domains, one from each gp41 monomer, bind in antiparallel orientation to the hydrophobic grooves of the coiled coil (9, 41, 43). Formation of helical bundles should bring the hydrophobic N-terminal domains referred to as fusion peptides and the C-terminal transmembrane domains (both not part of the crystal structure) to the same end of the rigid, rod-like molecule.

A large body of evidence indicates that the ability of gp41 to fold into a 6HB is critical for HIV Env-mediated fusion (reviewed in references 15 and 19). Most importantly, synthetic peptides derived from the N- and C-terminal heptad repeat domains of gp41 (referred to as N and C peptides, respectively) potently inhibit HIV entry and Env-induced membrane fusion (29, 33, 37, 44). It is widely accepted that N and C peptides block fusion by binding to their complementary regions on gp41 and preventing its folding into a 6HB (for an example, see reference 10). These peptides bind to gp41 intermediates formed after Env engages CD4, but they do not bind to a native conformation of the fusion protein (17, 18, 29) or to a 6HB (22). A set of gp41 conformations recognized by N or C peptides is collectively referred to as prebundles or prehairpins.

Because gp41 six-helix bundles likely represent the final, postfusion conformation (24, 29), it is important to identify the intermediate gp41 structures formed en route to a 6HB. The most commonly accepted two-step model of HIV fusion postulates the existence of gp41 intermediate that engages the target membrane by inserting the hydrophobic fusion peptides (10, 43) (Fig. 1). This intermediate conformation is thought to fold into a 6HB, bringing the fusion peptides and the transmembrane domains into close proximity and promoting membrane fusion. The first step of this model has been proposed by analogy to influenza hemagglutinin-induced fusion (14, 15, 39) for which insertion of fusion peptides into the target membrane prior to membrane merger has been experimentally demonstrated by a photoaffinity labeling technique (13, 40). However, this technique failed to detect a similar intermediate for HIV or simian immunodeficiency virus Env-induced fusion (35).

We have previously characterized conformational intermediates of gp41 by arresting HIV-1 Env-induced fusion at different stages and testing the ability of inhibitory peptides to block fusion from these intermediates (2, 24, 29). This analysis revealed two distinct sets of gp41 prebundle conformations—one that occurs before membrane merger and one that forms immediately after fusion pore opening. We obtained evidence

* Corresponding author. Present address: Institute of Human Virology, UMBI, 725 W. Lombard St., Baltimore, MD 21201. Phone: (410) 706-4781. Fax: (410) 706-4694. E-mail: melikian@umbi.umd.edu.

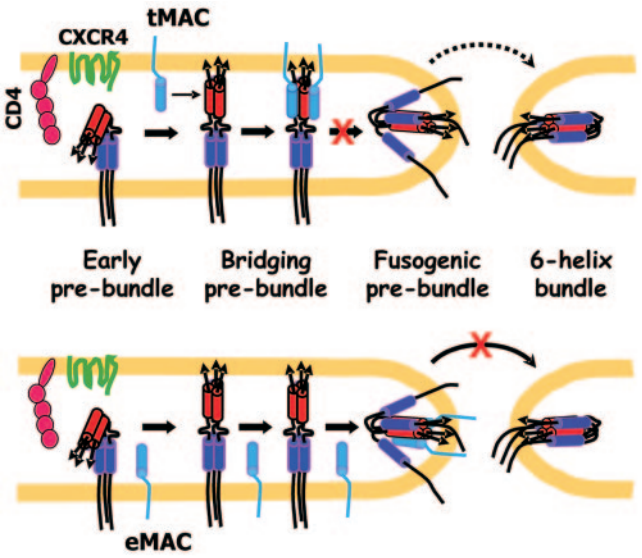

FIG. 1. A model of HIV Env-induced fusion and its inhibition by MACs. Intermediate conformations of gp41 are shown without gp120 for visual clarity. The C- and N-terminal heptad repeat domains are represented by blue and red cylinders, respectively. Fusion peptides are shown by arrows. Upper panel illustrates the proposed mechanism of inhibition by the tMACs, while the lower panel depicts the proposed mode of action of eMACs. The red X indicates the putative fusion step blocked by the peptides.

that gp41 prebundles are responsible for forming the pores, whereas 6HBs prevent pore closure and perhaps facilitate their enlargement (24). However, the utility of the inhibitory C peptides for further dissection of gp41 conformational changes is limited because these peptides do not discriminate between a multitude of prebundle conformations formed upstream of membrane merger.

In this work, we enabled selective binding of C peptides to a subset of gp41 prebundles by expressing these peptides in target cells (16, 21). The target membrane-anchored C peptides (tMACs) have been shown to bind soluble N peptides (derived from the gp41 coiled coil domain) and to inhibit infection and HIV-1 Env-induced cell fusion (16). A different study has shown that liposome-reconstituted trimeric gp41 fragments encompassing the C-helical and transmembrane domains also bind the N peptides and block HIV entry (23). Thus, both soluble and membrane-anchored C peptides (MACs) appear to inhibit fusion by binding to the coiled coil region of gp41 and preventing 6HB formation. However, based on topological considerations, tMACs must exclusively recognize gp41 conformations that bring the hydrophobic N termini of the trimeric coiled coil (known as fusion peptides) into close proximity with the target membrane (Fig. 1, upper panel). This proximity should almost assuredly lead to insertion of the hydrophobic fusion peptides into the target membrane, reducing the free energy of gp41 in this conformation. To determine whether gp41 engages the target membrane prior to fusion, we stabilized different conformations of gp41 by capturing fusion at distinct intermediate stages, followed by reestablishing the fusogenic conditions. Stabilizing gp41 conformations that are recognized by MACs would permit optimal binding and strongly potentiate the inhibitory activity of these peptides. Through this approach, we have identified an intermediate stage upstream of membrane merger that blocked subsequent fusion with MAC-expressing cells but not with target cells that lacked the peptide. These findings provide the first experimental evidence that formation of the target membrane-inserted conformation of HIV-1 gp41 is critical for fusion. This bridging conformation should effectively convert the energy released from the subsequent gp41 folding into a 6HB into a mechanical force that promotes membrane fusion.

MATERIALS AND METHODS

Cell lines and reagents. HEK293T cells were purchased from ATCC (Rockville, MD) and maintained in Dulbecco's modified Eagle's medium supplemented with 10% fetal calf serum and 0.5 mg/ml G418. PM-1/M87 and PM-1/M140 cells were derivatives of the parental PM-1 cell line engineered to express the membrane-anchored T20 (a 36-residue C peptide) and C46 peptides, respectively (16). For simplicity, we will refer to PM-1/M87 and PM-1/M140 cells as tT20 cells and tC46 cells, respectively. The control cells, PM-1/neo (designated PM-1), have been transduced with an empty vector (16). All three PM-1-derived cell lines were maintained in RPMI 1640 supplemented with 10% fetal calf serum and 0.8 mg/ml G418. Expression vector, peak10-syngp160mn, bearing a codon-optimized HIV MN Env gene (3), was a gift from Brian Seed (Massachusetts General Hospital). CD4 was transiently expressed from the pCDNA3 vector (provided by R. Doms, University of Pennsylvania), and the membrane-anchored C46 peptide was transiently expressed from the M87/C46-Ineo vector described previously (16). Synthetic C34 peptide derived from gp41 C-terminal heptad repeat region was purchased from Macromolecular Resources (Fort Collins, CO). The 12:0 lyso-phosphatidylcholine (LPC) was received from Avanti Polar Lipids (Alabaster, AL). Fluorescent dyes, calcein AM, CellTracker blue (7-amino-4-chloromethylcoumarin [CMAC]), and CellTracker green (5-chloromethylfluorescein diacetate [CMFDA]), were purchased from Molecular Probes (Eugene, OR). AMD3100 was purchased from Sigma Chemical (St. Louis, MO). The 2F5 antibody was kindly provided by H. Katinger and G. Stiegler. The following reagents were received from the NIAID AIDS Research and Reference Reagent Program (ARRRP): gp120 monoclonal antibody 2G12 (from Hermann Katinger) (7), CD4 monoclonal antibody SIM.4 (from J. Hildreth) (25), and AMD3100 (from AnorMed, Inc., Langley, British Columbia) (6, 12). We found that the latter batch of AMD3100 was less potent than the AMD3100 obtained from Sigma.

Expression of HIV Env, membrane-anchored C46, and CD4. Constitutive expression levels of tT20 and tC46 peptides in PM-1 cell lines were comparable, as has been shown by fluorescence-activated cell sorter analysis using 2F5 antibody (16). HIV Env (syngp160mn) was transiently expressed in HEK 293T cells by calcium phosphate transfection, using 5 μg of Env-expressing plasmid and 2.5 μg of cRev plasmid (a gift from Carol Weiss, FDA) per 60-mm dish, as described previously (28). The target 293T cells were transfected with 7 μg of CD4-encoding plasmid. When required, 2.5 μg of membrane-anchored C46 plasmid was added to the transfection mixture with Env and Rev or with CD4 expression vectors. The total amount of DNA in the transfection mixture was adjusted to 10 μg by adding appropriate amounts of an empty vector. Cell surface expression of HIV Env and CD4 (in the presence and absence of membrane-anchored C46 peptide) was determined by flow cytometry using human 2G12 (12 μg/5 × 10^5 cells) or mouse SIM.4 (1:10 dilution of hybridoma culture supernatant) monoclonal antibodies, respectively. Mock-transfected 293T cells and cells expressing HIV Env or CD4 were incubated with primary antibodies for 1 h at 4°C, washed, and incubated with phycoerythrin-conjugated goat anti-human or goat anti-mouse antibodies (Jackson ImmunoResearch, West Grove, PA), respectively. Cells were analyzed on an ORTHO Cytoron Absolute flow cytometer (Ortho Diagnostic Systems, Raritan, NJ).

Cell labeling and fusion experiments. Cells were loaded with fluorescent cytoplasmic dyes according to the manufacturer's instructions with slight modifications (29). 293T cells were labeled with green fluorescent dyes, calcein-AM, or CMFDA. The target cells (PM-1 or CD4-transfected 293T cells) were loaded with blue marker, CMAC. Effector and target cells were coincubated at 37°C, and the extent of cell fusion was quantified by visual observation in a fluorescent microscope (Zeiss Axiovert 200 M) using standard fluorescein isothiocyanate and 4′,6′-diamidino-2-phenylindole (DAPI) filter sets, as described in references (2 and 29). Briefly, several image fields were examined, and the number of double-positive (green/blue) cells was determined and normalized to the sum of fused and not fused effector/target (E/T) cell pairs. Approximately 100 cell pairs

were examined for each datum point. The kinetics of fusion was measured by adding a high concentration of C34 after different times of cell coincubation at 37°C. The temperature-arrested stage (TAS) (29) was created by coincubating the cells at 23°C for 2.5 h (unless otherwise indicated). The lipid-arrested stage (LAS) was created by treating the cells captured at TAS with 0.10 to 0.15 mg/ml LPC for 3 min at room temperature, followed by a 45-min incubation at 37°C in the presence of LPC. Fusion from LAS was induced by removing LPC from cell membranes by repetitive washing with cold Dulbecco's modified Eagle's medium supplemented with 0.1% bovine serum albumin and further incubating the cells at 37°C. Inhibition of fusion by AMD3100 was parameterized (to determine the 50% inhibitory concentration [IC_{50}]) by fitting the extent of fusion (F) as a function of drug concentration ([I]) to the following equation: $F = F_\infty + \{(F_0 - F_\infty)/(1 + [I]/IC_{50})\}$, where F_0 and F_∞ are the extents of fusion in the absence of AMD3100 and in the presence of an infinitely high concentration of the inhibitor, respectively.

RESULTS

Rationale. Synthetic soluble C peptides (e.g., T20 and C34) block fusion by binding to the hydrophobic grooves of the gp41 coiled coil transiently exposed in the course of fusion and preventing 6HB formation (see references 10 and 15 and references therein). Interactions of these peptides with the gp41 coiled coil should occur regardless of the position of gp41 with respect to the target membrane. In fact, C peptides bind to soluble CD4-triggered conformation(s) of gp41 (referred to as early prebundles) in the absence of target cells (17, 20, 29). To confer the ability to selectively recognize a subset of gp41 conformations that engage the target membrane, we engineered C peptides that were anchored to the target cell membrane through a single membrane-spanning domain (16, 21). We postulated that these spatially restricted peptides (referred to as tMACs) bind to the coiled coil domain of gp41 only when the N termini of these domains (i.e., the hydrophobic fusion peptides) are positioned against the target membrane (Fig. 1, upper panel). In this conformation, the fusion peptides are highly likely to insert into the target membrane, eliminating the prohibitively high energy of hydrophobic residues in an aqueous phase. In contrast, the topology of tMACs must prevent their interaction with early gp41 prebundles, e.g., those that form upon CD4 binding (17, 18, 29). We will hereafter refer to gp41 conformations that are recognized by tMACs as "bridging prebundles." Formation of heterologous complexes between MACs and bridging prebundles is expected to prevent 6HB formation and fusion (Fig. 1, upper panel).

If tMACs do selectively recognize a subset of prebundle conformations that engage the target membrane prior to membrane merger, three principal predictions can be made. First, tMACs are expected to arrest fusion at a stage that occurs after Env binds CD4 and coreceptor but before it induces hemifusion (merger of the contacting leaflets of two membranes without fusion pore formation) (27). Second, by analogy to soluble C peptides whose potency is determined by the time of gp41 prebundle exposure (2, 20, 36), the efficacy of tMACs should depend on the rate of conversion of bridging prebundles into 6HBs. In a 6HB conformation, gp41 no longer binds the C peptides, rendering fusion resistant to this class of inhibitors (22, 24). Hence, by reversibly arresting fusion at a stage where the bridging prebundles are formed, one should be able to optimize tMAC-gp41 interaction and achieve more potent inhibition of fusion compared to that upon direct coincubation at 37°C. Third, based on simple topological considerations (Fig. 1, lower panel), C peptides coexpressed with Env on effector cells (referred to as eMACs) should not interact with the bridging prebundles and, therefore, should not suppress fusion. Below we describe the experiments designed to test these predictions.

Target membrane-anchored C peptides delay the onset and decrease the extent of Env-induced fusion. To study the inhibition of fusion by tMACs, $CD4^+/CXCR4^+$ cells (PM-1 and their derivatives) were coincubated with effector cells transiently expressing X4-dependent HIV-1 Env. The extent and kinetics of fusion were quantified based on transfer of fluorescent aqueous dyes between cells, as described in references (29 and 30). Target cells either lacked (PM-1 cells) (Fig. 2) or stably expressed the T20 peptide (tT20 cells) or tC46 peptide (tC46 cells). The T20 peptide is comprised of the 36 membrane-proximal residues of the gp41 ectodomain (16), and the C46 peptide (tC46) encompasses 10 additional residues that are N-terminal to the T20 sequence. The latter residues are known to bind into the deep hydrophobic pocket within the gp41 coiled coil (8), contributing to the inhibitory activity of soluble C46. Expression of tT20 resulted in a relatively modest decrease of the extent of Env-induced fusion (Fig. 2A), whereas tC46 strongly suppressed fusion. It is worth pointing out that aqueous dye transfer to PM-1 cells occurred without appreciable delay, whereas fusion to tT20 and tC46 cells started after a significant lag time. In fact, tC46 cells did not fuse to effector cells during the first hour of coincubation at 37°C.

Notably, once started, fusion to PM-1, tT20, and tC46 cells occurred at the same rate. Indeed, normalizing the kinetics of aqueous dye transfer to the final extent of fusion and shifting the curves to compensate for their lag times yielded virtually superimposable kinetic curves for different target cells (Fig. 2B). To test whether soluble C peptides have the same effect on the fusion kinetics as tMACs, a suboptimal concentration of soluble C34 was added at the time of cell coculture. Soluble C34 increased the lag time to dye redistribution and reduced the fraction of fused cells (Fig. 2A) but did not significantly affect the rate of fusion after the lag time (Fig. 2B). Thus, the main kinetic effect of the soluble and membrane-anchored C peptides was elimination of the early fusion events. These effects on the kinetics and extent of fusion are consistent with reduction of density of fusion-competent Envs as a result of peptide binding. Note that lowering the number of activated Env by reducing the density of coreceptors on target membrane also delayed the onset of cell fusion (30).

tMACs capture gp41 conformations that occur upstream of membrane merger. Our model predicts that tMACs block fusion by binding to the bridging prebundles that engage the target membrane before the two membranes merge. We therefore tested whether fusion to cells expressing tMACs is blocked at the stage prior to hemifusion. Hemifusion is defined as the merger of contacting but not distal leaflets of two membranes that should result in transfer of lipophilic dye incorporated into the external lipid monolayer without redistribution of aqueous content (27). Generally, however, extensive internalization and segregation of lipophilic dyes inserted into the cell plasma membrane limits their utility for detecting cell-cell hemifusion. In addition, lipid diffusion through a local hemifusion site is restricted (1, 11, 26), further compromising the ability to detect a hemifusion intermediate. To determine whether hemifusion structures that restrict lipid mixing are

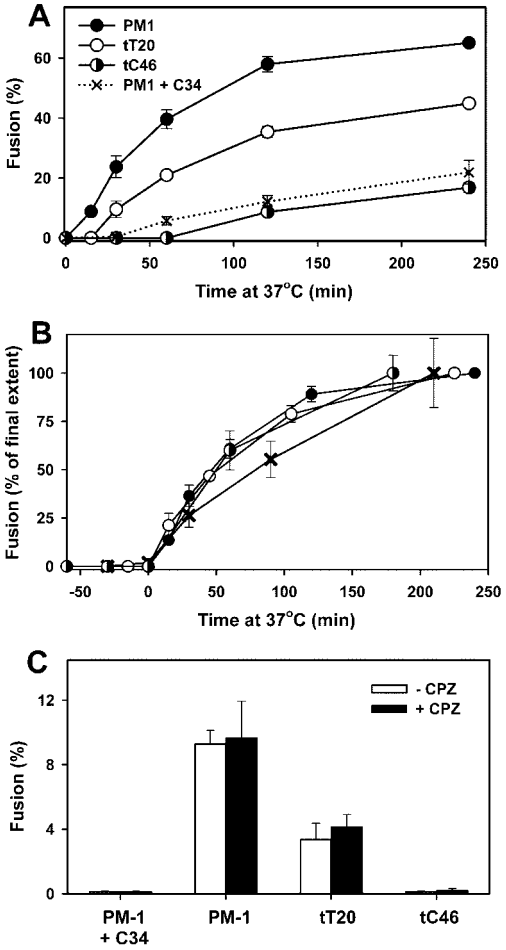

FIG. 2. The kinetics of HIV-1 Env-induced fusion to target PM-1 cells that do not express (filled circles) or express tT20 or tC46 (open and half-filled circles, respectively). (A) 293T cells transiently transfected with X4-tropic HIV Env (effector cells) were labeled with calcein, mixed with target cells loaded with CMAC, and coincubated at 37°C for varied times. Fusion was stopped at the indicated time intervals by adding 1 μM C34 peptide, and the extent of fusion was determined, as described in Materials and Methods. In control experiments, PM-1 cells were fused to effector cells in the presence of 75 nM of soluble C34 peptide (crosses). (B) Data from panel A were normalized to the extent of fusion after a 4-h incubation, and the curves were aligned at the onset of content mixing by subtracting the appropriate lag times to fusion. (C) The effect of chlorpromazine treatment (CPZ, filled bars) on fusion to target cells expressing (tT20 and tC46) or not expressing (PM-1) tMACs. Following a 30-min coincubation at 37°C, cells were treated with 0.5 mM CPZ in phosphate-buffered saline (PBS) for 1 min at room temperature, washed twice, and examined under a microscope. Control cells (open bars) were treated with PBS. Note that target cells were loaded with CMFDA instead of calcein to minimize the dye leakage caused by CPZ. To test whether hemifusion occurred in the presence of free C34, 1 μM C34 was added to the mixture of effector and target (PM-1) cells at the time of coculture (first column). Unless stated otherwise, the experimental points are means and standard errors of results from at least four independent experiments performed in duplicate.

formed with tMAC-expressing cells, we used chlorpromazine—an amphipathic drug that selectively destabilizes the hemifusion diaphragm and induces fusion (1, 26, 27). Target (PM-1, tT20, or tC46) and effector cell pairs were allowed to fuse for 30 min at 37°C and then briefly treated with 0.5 mM chlorpromazine. This treatment did not increase the extent of aqueous dye transfer compared to cells not exposed to chlorpromazine (Fig. 2C). We also found that the same treatment failed to induce fusion between E/T cells cocultured in the presence of high concentrations of C34 (Fig. 2C). These results suggest that both C34 and tMACs capture gp41 conformations that occur upstream of membrane merger.

tMACs block fusion at a stage that follows CD4 and coreceptor binding steps. It is widely accepted that C peptides bind exclusively to the gp41 coiled coil. However, there is evidence that soluble T20 (but not C34, for instance) associates with CD4-induced sites on X4-tropic gp120 and prevents gp120-CXCR4 binding (45). To address whether tT20 could also interfere with gp120-CXCR4 binding, we utilized a novel assay that monitors binding of Env on effector cells to CD4 and coreceptors on target cells in the absence of fusion (29, 30). This was achieved by prolonged coincubation of E/T cells at a temperature that was not permissive for fusion. Fusion from this TAS induced by warming cells to 37°C was partially resistant to CXCR4 and CCR5 binding inhibitors (30), implying that, for a fraction of E/T cells, a critical number of Envs have engaged a requisite number of coreceptor molecules. The degree of protection against coreceptor binding inhibitors increased with the time of preincubation. Thus, acquisition of resistance to coreceptor binding inhibitors at TAS provided a means to evaluate the rate and the extent of ternary (Env/CD4/coreceptor) complex formation.

We first measured the baseline sensitivity to a small-molecule CXCR4 binding inhibitor, AMD3100. The drug added at the beginning of cell coincubation at 37°C (referred to as "standard protocol") suppressed fusion to tT20-expressing cells much more potently than to PM-1 cells (Fig. 3A). The IC_{50} for PM-1 cells was almost an order of magnitude higher than that for tT20 cells (239 nM and 27 nM, respectively). In fact, a concentration of the drug that did not appreciably affect fusion to PM-1 cells (~100 nM) completely suppressed fusion to target cells expressing tT20. Thus, AMD3100 and tT20 greatly potentiate each other—a finding that is consistent with the previously observed synergism between soluble T20 and AMD3100 (42).

Next, we compared the extents and the rates of ternary complex formation with PM-1 and tT20 cells at subthreshold temperature. If tT20 interferes with gp120-CXCR4 binding, we expect that a larger fraction of cells expressing tT20 will be susceptible to AMD3100 inhibition at the TAS compared to cells lacking the peptide. With PM-1 cells as targets, a high concentration of the drug (greatly exceeding its IC_{90}) added at the TAS blocked about half of the fusion events that occurred in the absence of AMD3100 (Fig. 3B). Likewise, aqueous dye transfer to tT20 cells induced by raising temperature at the TAS was only partially blocked by AMD3100 added at this point (Fig. 3B). Thus, incubation at subthreshold temperature produced two distinct populations of E/T cells—one that was resistant and one that was sensitive to AMD3100 inhibition. Note that even the AMD3100-inhibitable population of tT20 cells demonstrated greatly (approximately sevenfold) increased resistance to the drug compared to that in a standard protocol (Fig. 3A and B). In fact, the IC_{50} for tT20 cells at the TAS (194 nM) was comparable to that for PM-1 cells (364 nM).

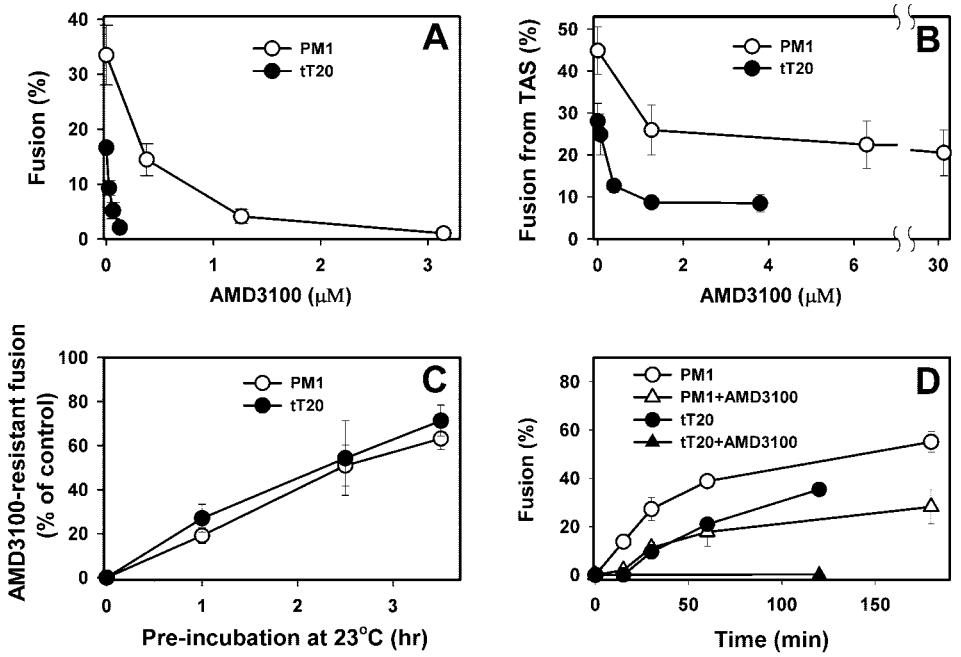

FIG. 3. Synergy between the inhibitory effects of tT20 and AMD3100. (A) Fusion to PM-1 and tT20 cells (open and filled circles, respectively) in the presence of varied concentrations of AMD3100. Cells were coincubated for 2 h at 37°C. (B) Inhibition of fusion by AMD3100 added at TAS. Effector cells were preincubated with PM-1 (open circles) or tT20 (filled circles) cells for 2.5 h at 23°C to create the TAS, treated with indicated concentrations of AM3100 (5 min at 23°C), and warmed to 37°C for 1 h. AMD3100 used for experiments in panels A and B was obtained through NIAID ARRRP. (C) PM-1 and tT20 cells (open and filled circles, respectively) were coincubated at 23°C with Env-expressing cells for 1, 2.5, or 3.5 h, followed by addition of 10 μM AMD3100 (obtained from Sigma) and further incubation for 1 h at 37°C. The acquisition of resistance to AMD3100 was expressed as the ratio of fusion in the presence of the drug to that in the absence of the drug. Experimental points are means ± standard errors of the means of results from two independent experiments performed in duplicate. (D) Kinetics of fusion to PM-1 and tT20 cells in the absence (open and filled circles, respectively) and in the presence (open and filled triangles) of 190 nM AMD3100 added at the beginning of cell coincubation at 37°C.

Partial protection against AMD3100 inhibition after an extended preincubation at 23°C (Fig. 3B) is consistent with slow assembly of gp120/CD4/CXCR4 complexes (30). We evaluated the rate of ternary complex formation by adding AMD3100 after varied times of preincubation at 23°C and found that these rates were virtually identical for PM-1 and tT20 cells (Fig. 3C). Also, in spite of the high AMD3100 sensitivity of tT20 cells in a standard protocol (Fig. 3A), comparable fractions of PM-1 and tT20 cells were resistant to the drug added at the TAS (Fig. 3B; Fig. 4A). Thus, neither the extent nor the rate of ternary complex formation was strongly affected by tMACs. We concluded that tMACs did not interfere with Env interactions with CD4 and coreceptors and that these peptides act at stages downstream of coreceptor binding steps.

The initial rate of fusion determines the potency of tMACs. The failure of tMACs to prevent ternary complex formation (Fig. 3B and C) rules out the possibility that tT20 interacts with coreceptor binding sites on gp120. Thus, tT20 does not synergize with AMD3100 by competing with coreceptors for binding to gp120. How does AMD3100 enhance the effect of tT20? Both the rate and the extent of HIV-1 Env-induced fusion are known to increase with the surface density of coreceptors (34, 36), whereas inhibitors of coreceptor binding prolong the lag time and reduce the efficacy of cell fusion and virus entry (30, 34). It is therefore likely that AMD3100 slows down the fusion reaction by reducing the density of CXCR4 available for Env activation and, thereby, permits more optimal tMAC-gp41 binding. In fact, for soluble C peptides, there is strong evidence that HIV resistance to these inhibitors is largely determined by the kinetics of fusion, which correlates with the rate of conversion into a final 6HB structure (2, 20, 36). Incomplete inhibition of cell fusion by tT20 (Fig. 2A) is consistent with the kinetically limited, inefficient binding to transiently formed gp41 bridging prebundles.

To validate the above mechanism, we measured the kinetics of content mixing in the presence of a moderate concentration (190 nM) of AMD3100 that reduced the extent of fusion by approximately twofold. Whereas the lag time to fusion with PM-1 cells in the absence of AMD3100 was negligibly small, the onset of dye transfer was delayed by ~15 min when a moderate dose of the inhibitor was present in the medium (Fig. 3D). This result is consistent with the idea that AMD3100 potentiates the effect of tMACs by reducing the rate of gp41 folding into a 6HB. As expected, the same moderate concentration of AMD3100 abolished fusion to tT20-expressing cells (Fig. 3D). The finding that the slower rate of fusion translated into more potent inhibition of fusion validates our strategy to identify the stage of fusion at which gp41 directly engages the target membrane by reversibly capturing the process at distinct intermediates upstream of membrane merger. If bridging prebundles are formed and captured at any of these intermediate stages, fusion induced by restoring the optimal conditions

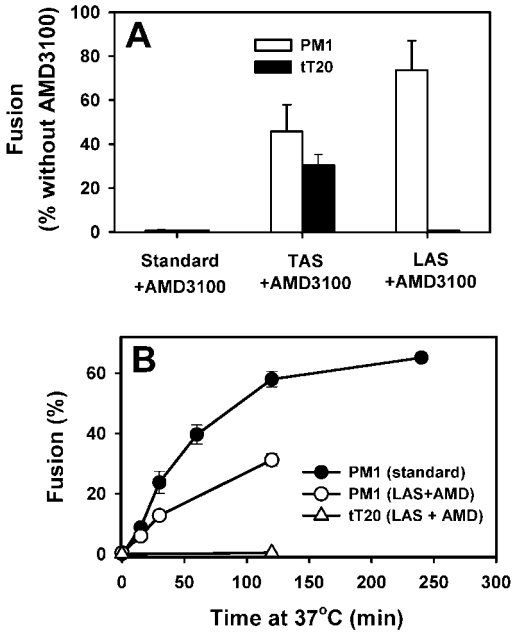

FIG. 4. Inhibitory potency of tMACs in a standard protocol and after arresting fusion at intermediate stages upstream of membrane merger. (A) HIV-1 Env-expressing 293T cells were fused to PM-1 (open bars) or tT20 (filled bars) cells. Fusion from the TAS (second column) and LAS (third column) was triggered in the presence of 20 μM AMD3100 (from NIAID ARRRP) to prevent dye transfer between cells that did not form ternary complexes at these stages (for details, see Materials and Methods). The extent of fusion was normalized to that obtained for PM-1 cells in the absence of AMD3100. (B) Kinetics of fusion to PM-1 cells (open circles) and tT20 cells (open triangles) induced by removing LPC (after arresting fusion at LAS) in the presence of 20 μM AMD3100 (NIAID ARRRP). The kinetics of fusion to PM-1 cells in a standard protocol is shown for comparison (filled circles, replotted from Fig. 2A).

from this point should be extremely sensitive to inhibition by tMACs.

gp41 does not engage the target membrane at temperature-arrested stage. Preincubation at 23°C (to create the TAS) did not significantly affect the extent of fusion compared to the standard protocol for both PM-1 and tT20 cells (Fig. 3A and B). Failure to improve the efficacy of tT20 upon creating the TAS suggests that gp41 does not form the bridging prebundles at this stage. However, to correctly determine the extent of fusion from this intermediate, it is important to prevent content mixing between E/T cell pairs that did not reach the TAS after preincubation at 23°C. Indeed, only a fraction of cells formed ternary complexes at this stage, as evidenced by partial protection against AMD3100 (Fig. 3B and C). Due to the heterogeneity of E/T cells captured at the TAS, dye transfer promoted by raising temperature can be induced by Env trimers that engaged CD4 and coreceptors, as well as by those that remained in their native state (referred to as "free" Env). To block fusion mediated by free Envs, a high concentration of AMD3100 was added before raising temperature to 37°C (Fig. 3B). To better illustrate the degree of AMD3100 resistance attained at the TAS, the fraction of cells fused in the presence of the drug was normalized to that in the absence of AMD3100 (Fig. 4A). Note that AMD3100 significantly reduced the extent of fusion from the TAS, demonstrating that the majority of fusion events that occurred from this stage (55% and 70% for PM-1 and tT20 cells, respectively) were, in fact, induced by free Envs. Because comparable fractions of both PM-1 and tT20 cells exhibited AMD3100-independent fusion from the TAS (Fig. 4A), we concluded that tT20 did not bind to Envs that engaged CD4 and coreceptors at subthreshold temperature. Thus, even though the gp41 coiled coils are likely exposed at the TAS (29), tMACs do not appear to interact with these structures. The lack of significant potentiation of tMAC activity at this stage led us to conclude that binding of gp120 to CD4 and coreceptors at subthreshold temperature is not sufficient to trigger gp41 refolding into bridging prebundles.

The bridging conformations of gp41 form at the lipid-arrested stage. To determine whether critical gp41 refolding that leads to target membrane engagement requires elevated temperature in addition to ternary complex formation, we tested the potency of tMACs after capturing fusion at the LAS. The LAS was created by exposing cells captured at TAS to 37°C in the presence of LPC—an inhibitory lipid that disfavors membrane rearrangements that lead to fusion (29). Aqueous dye redistribution from LAS was triggered by removing LPC and further incubating cells at 37°C (see Materials and Methods). As in TAS experiments, Envs that did not form ternary complexes with CD4 and coreceptors at LAS were prevented from inducing fusion by adding AMD3100. Cells were exposed to the drug immediately after LPC removal and prior to the final incubation at 37°C. The majority of PM-1 cells captured at LAS fused after optimal conditions were restored in the presence of AMD3100 (Fig. 4A), even though the drug was added at a concentration that exceeded that required to completely suppress fusion in a standard protocol (first column). In sharp contrast to PM-1 cells, fusion to tT20 cells did not occur in the presence of AMD3100 added at the LAS. Thus, tT20 appears to effectively capture the gp41 conformations formed at this stage, completely blocking their final refolding and membrane fusion that would otherwise have occurred upon removal of the inhibitory lipid. The finding that tMACs optimally recognize the intermediate structure(s) of gp41 formed at the LAS is consistent with formation of the bridging prebundles at this stage.

It is unlikely that fusion from the LAS was abolished due to tMACs interfering with the formation of ternary complexes because these complexes were already preformed at the TAS (Fig. 3B and C and 4A) and should not disassemble upon subsequent creation of the LAS (see Materials and Methods). In fact, ternary complex formation was further promoted at the LAS compared to the TAS for PM-1 cells, as evidenced by the increased fraction of cells that fused in the presence of AMD3100 (Fig. 4A). On the other hand, because the activity of tT20 has been strongly augmented when the initial rate of fusion was decreased by adding moderate doses of AMD3100 (Fig. 3D), it is conceivable that the effective block of fusion by tT20 from the LAS (Fig. 4A) occurred due to the slower kinetics of fusion from this stage. To address this possibility, we measured the kinetics of fusion to PM-1 and to tT20 cells (Fig. 4B) after arresting fusion at the LAS. Whereas the extent of fusion to PM-1 cells from the LAS was somewhat reduced, the overall rate of fusion was unaltered compared to fusion in a standard protocol. Most importantly, fusion from the LAS

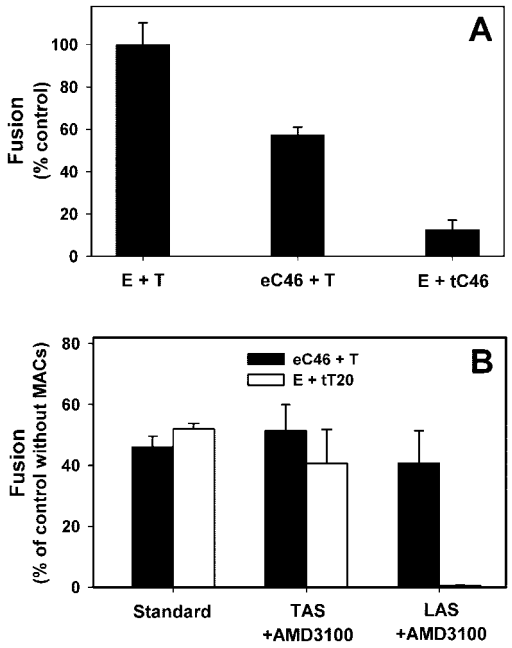

FIG. 5. The inhibitory activity of the membrane-anchored C46 expressed in effector (eC46) or in target (tC46) cells. (A) Fusion between 293T cells (E) expressing Env (loaded with green fluorescent dye, CMFDA) and 293T cells (T) transfected with CD4 (loaded with blue dye, CMAC) was quantified following 2 h of coculture at 37°C (first bar). The effect of C46 was evaluated by fusing target cells to effector cells coexpressing Env and C46 (eC46+T, second bar) or, alternatively, by fusing cells expressing Env to target cells that coexpressed CD4 and C46 (E+tC46, third bar). The extent of dye transfer was normalized to fusion between E/T cell pairs lacking the inhibitory peptide (first bar). (B) Dye transfer between 293T cells expressing Env and eC46 and target 293T cells expressing CD4 was measured in a standard protocol, after creating the TAS or LAS (eC46+T, filled bars). Fusion from the TAS and LAS was triggered in the presence of 20 μM AMD3100 (NIAID ARRRP). The data were normalized to the extent of fusion between target and effector cells lacking the inhibitory peptide. For comparison, the normalized extents of fusion between effector and tT20-expressing PM-1 cells are shown for all three fusion protocols (open bars).

started without a delay that could account for the increased potency of tMACs. In contrast, dye transfer to tT20 cells remained undetectable for several hours after lifting the block for fusion at the LAS (Fig. 4B). Thus, formation of gp41 bridging prebundles at LAS (Fig. 1) and their association with tMACs is the most likely explanation for the increased potency of tT20. We therefore concluded that engaging the target membrane at the LAS permitted optimal interaction between gp41 and tT20.

C peptides anchored to effector cells are poor inhibitors of Env-induced fusion. One of the principal predictions of our model was that, in contrast to tMACs, eMACs should not suppress fusion. To test this prediction, the C46 peptide was transiently coexpressed either with HIV Env in effector cells or with CD4 in target cells (designated eC46 and tC46, respectively). Because 293T cells expressed endogenous CXCR4, transfection with CD4 rendered them competent for fusion with Env-expressing cells (Fig. 5). However, it must be pointed out that considerable transfer of calcein occurred through gap junctions formed between the effector 293T and target 293T cell pairs in an Env- and receptor-independent manner (data not shown). Nonspecific dye redistribution was avoided by replacing calcein with CMFDA. CMFDA is a membrane-permeable thiol-reactive dye that is trapped in the cytoplasm after forming fluorescent thioether adducts; it did not transfer between 293T cells under nonfusogenic conditions (data not shown).

To meaningfully evaluate the inhibitory activity of membrane-anchored C46, the amounts of plasmids used for transfection were adjusted so that coexpression of the peptide did not reduce the level of CD4 or Env on the cell surface (Table 1). The level of C46 expression was not measured, but it was assumed that equal amounts of C46 plasmid yielded comparable expression in effector and in target 293T cells. In agreement with the results shown in Fig. 2, tC46 reduced the extent of CMFDA transfer by 10-fold (Fig. 5A). Surprisingly, when C46 was expressed in the effector membrane (eC46), the efficacy of fusion was significantly reduced (by ~40%) (Fig. 5A) compared to effector cells lacking the peptide. Thus, proper orientation of MACs with respect to the target membrane is important for their ability to block fusion, but the peptides coexpressed with Env can also exhibit appreciable inhibitory activity.

eMACs likely target postfusion conformations of gp41. The finding that effector cell-anchored peptides attenuate HIV-1 Env-induced fusion activity raises several questions. Do tMACs and eMACs block fusion by the same fundamental mechanism? If not, what steps of the fusion reaction are targeted by eMACs? eMACs expressed in effector cells should not be able to recognize gp41 bridging prebundles (Fig. 1). If these peptides bind to any other conformations of gp41 downstream of coreceptor binding but upstream of membrane merger, the efficacy of inhibition by eMACs should be altered by temporarily arresting fusion at intermediate stages that precede membrane merger (as was the case for the tT20 peptide) (Fig. 4A). We therefore determined whether capturing fusion at the TAS or LAS affected the ability of eC46 to inhibit fusion. To prevent dye transfer induced by Envs that did not bind CD4 and CXCR4 at these stages, cells were exposed to AMD3100 before restoration of the fusogenic conditions. The extent of dye transfer between the target cells and effector cells expressing eC46 was measured for different fusion protocols and normalized to fusion with effector cells lacking the inhibitory peptide (Fig. 5B). We found that the relative efficacy of eC46 was not affected by the exact protocol

TABLE 1. Coexpression of HIV Env or CD4 with membrane-anchored C46 construct in 293T cells[a]

Transfected construct(s)	% Positive cells[b]	MCF[c] (% of control)
Env (5 μg)	12.3	100
Env (5 μg) + eC46 (2.5 μg)	18.6	110
CD4 (7 μg)	65.7	100
CD4 (7 μg) + tC46 (2.5 μg)	81.5	129

[a] Env, CD4, and membrane-anchored C46 were expressed in 293T cells by transient transfection, as described in Materials and Methods. Mean values of the results from two independent measurements are shown.

[b] Percentage of cells stained with antibodies (for details, see Materials and Methods).

[c] Mean channel fluorescence.

used to induce fusion. This result was in contrast to that of tMAC-expressing cells that were rendered fusion incompetent, following creation of the LAS (Fig. 4A). To better illustrate this point, we replotted data from Fig. 4A after normalizing fusion with tT20 cells to fusion with PM-1 cells (Fig. 5B). Because arresting fusion at steps prior to membrane merger did not lead to significant changes in eMAC activity, we hypothesized that these peptides target gp41 prebundles formed after fusion pore opening.

To further examine which steps of fusion are targeted by eMACs, additional experiments were performed, this time, with PM-1 cells as targets. First, we determined whether eC46 can selectively bind early conformational intermediates of gp41 induced by receptor binding. To this end, effector cells were treated with soluble CD4 (sCD4). Binding of gp120 to sCD4 is known to induce exposure/formation of the gp41 coiled coil domain (17, 29) and to compromise the fusogenic activity of HIV Env through sCD4-induced gp120 shedding or other mechanisms (31, 32). If the coiled coil domain exposed after sCD4 treatment is positioned in the vicinity of the Env-expressing membrane with its N terminus facing that membrane (Fig. 1, early prebundle), eC46 can conceivably bind gp41 and impair further conformational changes leading to fusion. Effector cells expressing or not expressing eC46 were pretreated with sCD4, washed to remove unbound receptor, and cocultured with PM-1 cells (Fig. 6A). If eMACs recognized sCD4-induced conformations of gp41, they would be expected to further potentiate the effect of sCD4. However, pretreatment with sCD4 reduced fusion to effector cells lacking eC46 and to those expressing eC46 to a similar extent. Thus, eC46 does not appear to interact with early gp41 prebundles that are formed as a result of CD4 binding.

Next, we asked whether eMACs can interfere with the subsequent step of fusion: formation of ternary Env/CD4/CXCR4 complexes. As described above (Fig. 3C), ternary complex formation was detected by probing the ability of AMD3100 to block cell fusion after varied times of preincubation at subthreshold temperature. The rate of increase in the extent of AMD3100-resistant fusion upon preincubation at 23°C was very close for effector cells lacking and those expressing the eC46 peptide (Fig. 6B). These results, combined with data shown in Fig. 3C, show that neither eMACs nor tMACs interfere with gp120 binding to CD4 and coreceptors.

Finally, we determined whether eC46 synergizes with AMD3100, as has been documented for tT20 (Fig. 3A and 6C). We found that eC46-expressing cells were as resistant to AMD3100 inhibition as effector cells lacking the peptide (Fig. 6C), showing that the drug did not potentiate eMAC activity. Collectively, our data support the conclusion that eMACs do not recognize gp41 conformations upstream of membrane merger, so they must bind to late gp41 prebundles around the fusion pore.

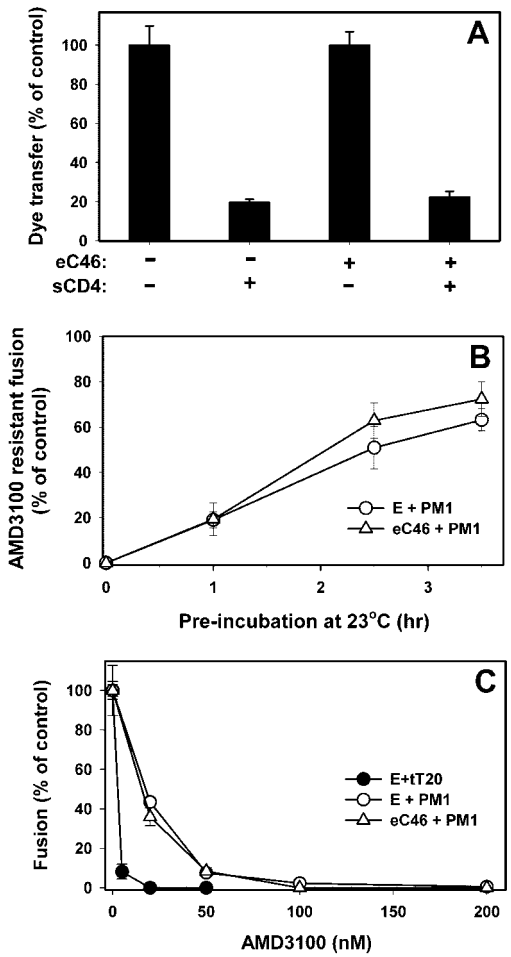

FIG. 6. Inhibitory activity of C46 anchored to effector cell membrane (eC46). (A) Effector cells either not expressing (first and second bar) or expressing (third and fourth bar) the eC46 were pretreated with 7 μg/ml sCD4 (10 min, 37°C), washed twice, and coincubated with PM-1 cells for 2 h at 37°C. The effect of sCD4 on fusion was quantified by normalizing the fraction of fused cells to that in the absence of the soluble receptor. (B) Effector cells lacking (circles) or expressing (triangles) eC46 were coincubated with PM-1 cells at 23°C for varied times, exposed to 10 μM AMD3100, and warmed to 37°C. The acquisition of resistance to AMD3100 is expressed as the ratio of fusion in the presence of AMD3100 to that in the absence of the drug. Experimental points are means ± standard errors of the means of results from two independent experiments performed in duplicate. (C) Dose dependences of inhibition of fusion between control cells lacking MACs (E+PM1, open circles), between eC46-expressing and PM-1 cells (eC46+PM1, open triangles), or between effector and tT20-expressing cells (E+tT20, filled circles). The data were normalized to fusion in the absence of the drug. AMD3100 used in the experiments for which results are shown in Fig. 6 was purchased from Sigma.

DISCUSSION

HIV-1 gp41 engages the target membrane before inducing fusion. In this work, tMACs were utilized to identify the gp41 conformations that bridge the viral and target membranes prior to fusion. Our strategy was based on two assumptions. First, we postulated that tMACs bind exclusively to the target membrane-engaged (bridging) conformations of gp41 but not to early gp41 prebundles (Fig. 1). Second, we assumed that, by analogy to soluble C peptides (2, 20, 36), the potency of tMACs is determined primarily by the lifetime of gp41 prebundles targeted by these peptides. Thus, in the case of tMACs, the longevity of bridging prebundles is the major determinant of their inhibitory activity. We attempted to increase the time of bridging prebundle exposure by reversibly capturing fusion at intermediate stages upstream of membrane merger (TAS and LAS). We then looked for a qualitative potentiation of tMAC

activity, which was taken to indicate that stable bridging prebundles had formed at that stage.

We have recently investigated the effect of arresting fusion at the TAS or LAS on the ability of soluble C34 to inhibit cell-cell fusion induced by X4-tropic HIV-1 Env (2). Surprisingly, capturing fusion at these intermediate stages did not significantly alter the inhibitory concentrations of C34 compared to direct incubation at 37°C. This finding argues that, under our experimental conditions, the overall time spent in prebundle conformations was sufficiently long to ensure optimal peptide binding. In contrast to soluble C34, tMAC inhibitory activity was greatly improved after arresting fusion at the LAS (Fig. 4A). This important result implies that the bridging prebundles are normally too short-lived to allow optimal binding of tMACs and that these structures can be stabilized at 37°C in the presence of inhibitory lipids. On the other hand, the lack of augmentation of tMAC activity after preincubation at subthreshold temperature (TAS) is consistent with our initial assumption that tMACs do not recognize early gp41 prebundles upstream of the bridging conformation. In summary, this work provides experimental evidence that, following CD4 and coreceptor binding, HIV-1 gp41 inserts its fusion peptides into the target membrane—a critical step that mechanically couples further refolding of gp41 into a 6HB and membrane merger.

It is worth pointing out that, in contrast to photoaffinity labeling techniques (for examples, see references 13 and 40) that directly detect the target membrane-engaged conformations of fusion proteins upstream of membrane merger, the functional approach employed in this paper is rather indirect. On the other hand, the photoaffinity labeling can potentially reveal structures forming as a result of a concurrent off-path reaction that does not lead to productive fusion. The distinct advantage of fusion assays is that they, by definition, pertain to the proteins involved in the productive fusion. The ability of tMACs to completely block dye redistribution between cells under conditions that permit optimal binding to gp41 prebundles (most likely the bridging prebundles) demonstrates that formation of these prebundles and their conversion to six-helix bundles is critical for fusion. Thus, our results, for the first time, provide evidence that bridging prebundles are bona fide intermediates of gp41-induced fusion.

Possible mechanism of inhibition by MACs expressed in effector cells. Based on the position and orientation of eMACs with respect to gp41, we envisioned that these peptides would not bind to gp41 and, therefore, would not inhibit fusion. Surprisingly, however, we found that eMACs exhibited weak inhibitory activity (Fig. 5A). This effect was not related to reduction in Env expression (Table 1) nor was it due to interactions with gp41 intermediates formed upstream of membrane merger (Fig. 6). The lack of eMAC-gp41 interactions prior to membrane merger is supported by the following observations. First, eC46 did not appear to recognize gp41 structures formed after Env-sCD4 binding at 37°C or after formation of ternary Env/CD4/CXCR4 complexes at subthreshold temperature (Fig. 6A and 5B, respectively). Second, in contrast to tT20, eC46 activity was not potentiated by a moderate concentration of AMD3100 that slows down the fusion reaction (Fig. 6C). Third, the efficacy of eC46 did not increase after capturing fusion at the LAS (Fig. 5B), a stage that immensely improved the potency of tMACs.

To account for the above results, we propose that eMACs bind to gp41 prebundles around the fusion pore by diffusing laterally along the pore walls and properly positioning themselves with respect to the coiled coil domain (Fig. 1, lower panel). We envision that, by interacting with the fusogenic gp41 prebundles around the nascent pore, eMACs can induce pore closure. The poor inhibitory effect of eC46 (Fig. 5) is consistent with a low efficacy of binding to transient gp41 prebundles involved in pore formation. An alternative possibility is that eMACs somehow associate with the native form of gp41, rendering it inactive. However, to our knowledge, binding between the viral membrane-proximal region of gp41 and C peptides has not been documented.

Formation of ternary gp120/CD4/CXCR4 complexes is necessary but not sufficient to trigger gp41-induced fusion. We have previously shown that gp41 prebundles are formed at the TAS (29). At this point, gp120 binds CD4 and, at least partially, engages CXCR4 (Fig. 3C and 6B) (30). Clearly, however, binding to CD4 and coreceptors at subthreshold temperature is not sufficient to induce fusion (2, 30). Moreover, the tMAC-based approach utilized in this paper revealed that formation of ternary complexes at 23°C (TAS) did not appear to promote insertion of the gp41 fusion peptides into the target membrane. This finding is in agreement with the lack of direct gp41-target membrane interactions at subthreshold temperature documented by the photoaffinity labeling technique (35). Because optimal interactions between tMACs and gp41 occur at the LAS but not at the TAS (Fig. 4A), it is most likely that insertion of the gp41 fusion peptides into the target membrane is triggered by raising the temperature from the TAS. To conclude, the combination of ternary complex formation and elevated temperature is a prerequisite for gp41 refolding that leads to engagement of the target membrane and, ultimately, induces membrane fusion.

The markedly increased potency of tMACs after creation of the lipid-arrested stage implies that, once formed, the bridging conformation of gp41 can be stabilized at 37°C in the presence of inhibitory lipids. These and other stabilized fusion intermediates can present new targets for antiviral drugs. By engineering a disulfide bond between gp120 and gp41 subunits, we and others have previously captured another fusion intermediate upstream of membrane merger (1, 4). The mutant Env, termed SOS (5), engaged CD4 and coreceptors upon coculture with target cells at 37°C but did not induce fusion. From this stage, fusion could be triggered by reducing the intersubunit disulfide bond with dithiothreitol. We predicted that SOS-induced fusion was captured at an advanced stage where Envs formed the bridging prebundles (1). This notion can now be tested by using the tMAC-based experimental approach developed in the present work.

ACKNOWLEDGMENTS

We thank Lev Deriy for excellent technical support, Leonid Chernomordik and Sergey Cheresiz for critical reading of the manuscript, Greg Spear for the use of his flow cytometer, and Brian Seed for providing the codon-optimized HIV Env plasmid. We are also grateful to the NIH ARRRP for providing the reagents.

This work was supported by NIH grant GM54787 to G.B.M. and the European Commission project TRIoH LSHG-CT-2003 grant to D.V.L.

REFERENCES

1. **Abrahamyan, L. G., R. M. Markosyan, J. P. Moore, F. S. Cohen, and G. B. Melikyan.** 2003. Human immunodeficiency virus type 1 Env with an intersubunit disulfide bond engages coreceptors but requires bond reduction after engagement to induce fusion. J. Virol. **77:**5829–5836.
2. **Abrahamyan, L. G., S. R. Mkrtchyan, J. Binley, M. Lu, G. B. Melikyan, and F. S. Cohen.** 2005. The cytoplasmic tail slows the folding of human immunodeficiency virus type 1 Env from a late prebundle configuration into the six-helix bundle. J. Virol. **79:**106–115.
3. **Andre, S., B. Seed, J. Eberle, W. Schraut, A. Bultmann, and J. Haas.** 1998. Increased immune response elicited by DNA vaccination with a synthetic gp120 sequence with optimized codon usage. J. Virol. **72:**1497–1503.
4. **Binley, J. M., C. S. Cayanan, C. Wiley, N. Schulke, W. C. Olson, and D. R. Burton.** 2003. Redox-triggered infection by disulfide-shackled human immunodeficiency virus type 1 pseudovirions. J. Virol. **77:**5678–5684.
5. **Binley, J. M., R. W. Sanders, B. Clas, N. Schuelke, A. Master, Y. Guo, F. Kajumo, D. J. Anselma, P. J. Maddon, W. C. Olson, and J. P. Moore.** 2000. A recombinant human immunodeficiency virus type 1 envelope glycoprotein complex stabilized by an intermolecular disulfide bond between the gp120 and gp41 subunits is an antigenic mimic of the trimeric virion-associated structure. J. Virol. **74:**627–643.
6. **Bridger, G. J., R. T. Skerlj, D. Thornton, S. Padmanabhan, S. A. Martellucci, G. W. Henson, M. J. Abrams, N. Yamamoto, K. De Vreese, R. Pauwels, et al.** 1995. Synthesis and structure-activity relationships of phenylenebis(methylene)-linked bis-tetraazamacrocycles that inhibit HIV replication. Effects of macrocyclic ring size and substituents on the aromatic linker. J. Med. Chem. **38:**366–378.
7. **Buchacher, A., R. Predl, K. Strutzenberger, W. Steinfellner, A. Trkola, M. Purtscher, G. Gruber, C. Tauer, F. Steindl, A. Jungbauer, et al.** 1994. Generation of human monoclonal antibodies against HIV-1 proteins; electrofusion and Epstein-Barr virus transformation for peripheral blood lymphocyte immortalization. AIDS Res. Hum. Retrovir. **10:**359–369.
8. **Chan, D. C., C. T. Chutkowski, and P. S. Kim.** 1998. Evidence that a prominent cavity in the coiled coil of HIV type 1 gp41 is an attractive drug target. Proc. Natl. Acad. Sci. USA **95:**15613–15617.
9. **Chan, D. C., D. Fass, J. M. Berger, and P. S. Kim.** 1997. Core structure of gp41 from the HIV envelope glycoprotein. Cell **89:**263–273.
10. **Chan, D. C., and P. S. Kim.** 1998. HIV entry and its inhibition. Cell **93:**681–684.
11. **Chernomordik, L. V., V. A. Frolov, E. Leikina, P. Bronk, and J. Zimmerberg.** 1998. The pathway of membrane fusion catalyzed by influenza hemagglutinin: restriction of lipids, hemifusion, and lipidic fusion pore formation. J. Cell Biol. **140:**1369–1382.
12. **De Clercq, E., N. Yamamoto, R. Pauwels, J. Balzarini, M. Witvrouw, K. De Vreese, Z. Debyser, B. Rosenwirth, P. Peichl, R. Datema, et al.** 1994. Highly potent and selective inhibition of human immunodeficiency virus by the bicyclam derivative JM3100. Antimicrob. Agents Chemother. **38:**668–674.
13. **Durrer, P., C. Galli, S. Hoenke, C. Corti, R. Gluck, T. Vorherr, and J. Brunner.** 1996. H^+-induced membrane insertion of influenza virus hemagglutinin involves the HA2 amino-terminal fusion peptide but not the coiled coil region. J. Biol. Chem. **271:**13417–13421.
14. **Earp, L. J., S. E. Delos, H. E. Park, and J. M. White.** 2005. The many mechanisms of viral membrane fusion proteins. Curr. Top. Microbiol. Immunol. **285:**25–66.
15. **Eckert, D. M., and P. S. Kim.** 2001. Mechanisms of viral membrane fusion and its inhibition. Annu. Rev. Biochem. **70:**777–810.
16. **Egelhofer, M., G. Brandenburg, H. Martinius, P. Schult-Dietrich, G. Melikyan, R. Kunert, C. Baum, I. Choi, A. Alexandrov, and D. von Laer.** 2004. Inhibition of human immunodeficiency virus type 1 entry in cells expressing gp41-derived peptides. J. Virol. **78:**568–575.
17. **Furuta, R. A., C. T. Wild, Y. Weng, and C. D. Weiss.** 1998. Capture of an early fusion-active conformation of HIV-1 gp41. Nat. Struct. Biol. **5:**276–279.
18. **Gallo, S. A., G. M. Clore, J. M. Louis, C. A. Bewley, and R. Blumenthal.** 2004. Temperature-dependent intermediates in HIV-1 envelope glycoprotein-mediated fusion revealed by inhibitors that target N- and C-terminal helical regions of HIV-1 gp41. Biochemistry **43:**8230–8233.
19. **Gallo, S. A., C. M. Finnegan, M. Viard, Y. Raviv, A. Dimitrov, S. S. Rawat, A. Puri, S. Durell, and R. Blumenthal.** 2003. The HIV Env-mediated fusion reaction. Biochim. Biophys. Acta **1614:**36–50.
20. **Gallo, S. A., K. Sackett, S. S. Rawat, Y. Shai, and R. Blumenthal.** 2004. The stability of the intact envelope glycoproteins is a major determinant of sensitivity of HIV/SIV to peptidic fusion inhibitors. J. Mol. Biol. **340:**9–14.
21. **Hildinger, M., M. T. Dittmar, P. Schult-Dietrich, B. Fehse, B. S. Schnierle, S. Thaler, G. Stiegler, R. Welker, and D. von Laer.** 2001. Membrane-anchored peptide inhibits human immunodeficiency virus entry. J. Virol. **75:**3038–3042.
22. **Kliger, Y., and Y. Shai.** 2000. Inhibition of HIV-1 entry before gp41 folds into its fusion-active conformation. J. Mol. Biol. **295:**163–168.
23. **Lenz, O., M. T. Dittmar, A. Wagner, B. Ferko, K. Vorauer-Uhl, G. Stiegler, and W. Weissenhorn.** 2005. Trimeric membrane-anchored gp41 inhibits HIV membrane fusion. J. Biol. Chem. **280:**4095–4101.
24. **Markosyan, R. M., F. S. Cohen, and G. B. Melikyan.** 2003. HIV-1 envelope proteins complete their folding into six-helix bundles immediately after fusion pore formation. Mol. Biol. Cell **14:**926–938.
25. **McCallus, D. E., K. E. Ugen, A. I. Sato, W. V. Williams, and D. B. Weiner.** 1992. Construction of a recombinant bacterial human CD4 expression system producing a bioactive CD4 molecule. Viral Immunol. **5:**163–172.
26. **Melikyan, G. B., R. J. Barnard, R. M. Markosyan, J. A. Young, and F. S. Cohen.** 2004. Low pH is required for avian sarcoma and leukosis virus Env-induced hemifusion and fusion pore formation but not for pore growth. J. Virol. **78:**3753–3762.
27. **Melikyan, G. B., S. A. Brener, D. C. Ok, and F. S. Cohen.** 1997. Inner but not outer membrane leaflets control the transition from glycosylphosphatidylinositol-anchored influenza hemagglutinin-induced hemifusion to full fusion. J. Cell Biol. **136:**995–1005.
28. **Melikyan, G. B., R. M. Markosyan, S. A. Brener, Y. Rozenberg, and F. S. Cohen.** 2000. Role of the cytoplasmic tail of ecotropic moloney murine leukemia virus Env protein in fusion pore formation. J. Virol. **74:**447–455.
29. **Melikyan, G. B., R. M. Markosyan, H. Hemmati, M. K. Delmedico, D. M. Lambert, and F. S. Cohen.** 2000. Evidence that the transition of HIV-1 gp41 into a six-helix bundle, not the bundle configuration, induces membrane fusion. J. Cell Biol. **151:**413–424.
30. **Mkrtchyan, S. R., R. M. Markosyan, M. T. Eadon, J. P. Moore, G. B. Melikyan, and F. S. Cohen.** 2005. Ternary complex formation of human immunodeficiency virus type 1 Env, CD4, and chemokine receptor captured as an intermediate of membrane fusion. J. Virol. **79:**11161–11169.
31. **Moore, J. P., J. A. McKeating, W. A. Norton, and Q. J. Sattentau.** 1991. Direct measurement of soluble CD4 binding to human immunodeficiency virus type 1 virions: gp120 dissociation and its implications for virus-cell binding and fusion reactions and their neutralization by soluble CD4. J. Virol. **65:**1133–1140.
32. **Moore, J. P., J. A. McKeating, R. A. Weiss, and Q. J. Sattentau.** 1990. Dissociation of gp120 from HIV-1 virions induced by soluble CD4. Science **250:**1139–1142.
33. **Munoz-Barroso, I., S. Durell, K. Sakaguchi, E. Appella, and R. Blumenthal.** 1998. Dilation of the human immunodeficiency virus-1 envelope glycoprotein fusion pore revealed by the inhibitory action of a synthetic peptide from gp41. J. Cell Biol. **140:**315–323.
34. **Platt, E. J., J. P. Durnin, and D. Kabat.** 2005. Kinetic factors control efficiencies of cell entry, efficacies of entry inhibitors, and mechanisms of adaptation of human immunodeficiency virus. J. Virol. **79:**4347–4356.
35. **Raviv, Y., M. Viard, J. Bess, Jr., and R. Blumenthal.** 2002. Quantitative measurement of fusion of HIV-1 and SIV with cultured cells using photosensitized labeling. Virology **293:**243–251.
36. **Reeves, J. D., S. A. Gallo, N. Ahmad, J. L. Miamidian, P. E. Harvey, M. Sharron, S. Pohlmann, J. N. Sfakianos, C. A. Derdeyn, R. Blumenthal, E. Hunter, and R. W. Doms.** 2002. Sensitivity of HIV-1 to entry inhibitors correlates with envelope/coreceptor affinity, receptor density, and fusion kinetics. Proc. Natl. Acad. Sci. USA **99:**16249–16254.
37. **Root, M. J., M. S. Kay, and P. S. Kim.** 2001. Protein design of an HIV-1 entry inhibitor. Science **291:**884–888.
38. **Skehel, J. J., and D. C. Wiley.** 1998. Coiled coils in both intracellular vesicle and viral membrane fusion. Cell **95:**871–874.
39. **Stegmann, T.** 2000. Membrane fusion mechanisms: the influenza hemagglutinin paradigm and its implications for intracellular fusion. Traffic **1:**598–604.
40. **Stegmann, T., J. M. Delfino, F. M. Richards, and A. Helenius.** 1991. The HA2 subunit of influenza hemagglutinin inserts into the target membrane prior to fusion. J. Biol. Chem. **266:**18404–18410.
41. **Tan, K., J. Liu, J. Wang, S. Shen, and M. Lu.** 1997. Atomic structure of a thermostable subdomain of HIV-1 gp41. Proc. Natl. Acad. Sci. USA **94:**12303–12308.
42. **Tremblay, C. L., C. Kollmann, F. Giguel, T. C. Chou, and M. S. Hirsch.** 2000. Strong in vitro synergy between the fusion inhibitor T-20 and the CXCR4 blocker AMD-3100. J. Acquir. Immune Defic. Syndr. **25:**99–102.
43. **Weissenhorn, W., A. Dessen, S. C. Harrison, J. J. Skehel, and D. C. Wiley.** 1997. Atomic structure of the ectodomain from HIV-1 gp41. Nature **387:**426–430.
44. **Wild, C., T. Greenwell, and T. Matthews.** 1993. A synthetic peptide from HIV-1 gp41 is a potent inhibitor of virus-mediated cell-cell fusion. AIDS Res. Hum. Retrovir. **9:**1051–1053.
45. **Yuan, W., S. Craig, Z. Si, M. Farzan, and J. Sodroski.** 2004. CD4-induced T-20 binding to human immunodeficiency virus type 1 gp120 blocks interaction with the CXCR4 coreceptor. J. Virol. **78:**5448–5457.